Photodiagnosis and Photodynamic Therapy 25 (2019) 7–16

Contents lists available at ScienceDirect

Photodiagnosis and Photodynamic Therapy

journal homepage: www.elsevier.com/locate/pdpdt

Antimicrobial efficacy of methylene blue-mediated photodynamic therapy on titanium alloy surfaces *in vitro*

Tsun-Chin Huang[a], Chun-Ju Chen[a], Shinn-Jyh Ding[a,b,*], Chun-Cheng Chen[b,c,**]

[a] Institute of Oral Science, Chung Shan Medical University, Taichung City 402, Taiwan
[b] Department of Stomatology, Chung Shan Medical University Hospital, Taichung City 402, Taiwan
[c] School of Dentistry, Chung Shan Medical University, Taichung City 402, Taiwan

ARTICLE INFO

Keywords:
Peri-implantitis
Photodynamic therapy
Methylene blue
Antimicrobial activity
Lipopolysaccharide
Antimicrobial photodynamic therapy

ABSTRACT

Bacterial elimination using antimicrobial photodynamic therapy (aPDT) has been considered an alternative therapeutic modality in peri-implantitis treatment. The present in vitro study evaluated the dose-dependent and pH-dependent bactericidal effects of methylene blue (MB)-mediated aPDT at eliminating Gram-negative (*P. gingivalis* and *A. actinomycetemcomitans*) and Gram-positive (*S. mutans*) bacteria on sandblasting, large-grit and acid-etching (SLA)-pretreated titanium alloy. The effects of different MB concentrations (50, 100, and 200 μg/mL), the pH of the MB (4, 7, and 10), and irradiation time (0, 30, and 60 s) on the bacterial viability and residual lipopolysaccharide (LPS) levels were examined. The variations in the pH of the MB solution after aPDT for 60 s on the uncontaminated and contaminated specimens were also detected. The experimental results indicated that MB-mediated PDT could effectively kill the majority of bacteria on the titanium alloy surfaces of biofilm-contaminated implants compared with the MB alone. Of note, aPDT exhibited better antibacterial efficacy with increase in the MB concentration and irradiation time. While treated in an acidic solution on the biofilm-contaminated specimens, aPDT caused the pH to increase. By contrast, the initially high alkaline pH decreased to a value of about pH 8.5 after aPDT. Intriguingly, the neutral pH had minor changes, independent of the MB concentration and bacterial species. As expected, aPDT with higher MB concentration at higher pH environment significantly lowered the LPS concentration of *A. actinomycetemcomitans* and *P. gingivalis*. On the basis of the data, the aPDT with 200 μg/mL MB at pH 10 for 60 s of irradiation time might be an effectively treatment to eliminate bacteria and LPS adherent to titanium surface, however, the use of the multispecies biofilm model and the evaluation of in vitro osteogenesis needed to be further evaluated.

1. Introduction

Microbial biofilms play a vital role in the development of dental caries, periodontitis, and peri-implant diseases [1–3]. The formation of polysaccharide matrix-enclosed biofilms is based to the intricate interactions between a surface and microbial cells. In particular, insoluble polysaccharides favor the formation of dental plaque, biofilm stability, and structural integrity, which are less susceptible to antimicrobial agents [4–6]. Among biofilm-associated diseases, peri-implantitis could result in the pocket formation and loss of supporting bone during the destructive inflammatory process [7]. Peri-implantitis has been estimated to take place in 10.7–47.2% of dental implant patients within 10 years of post-treatment observation [8]. The major purpose of peri-implantitis therapy has been to eliminate all bacterial deposits on the implant surface. Although several debridement methods such as mechanical debridement have been reported for the treatment of peri-implantitis, some of them would damage the implant surface [9]. For example, air-powder abrasive system effectively eradicates surface contamination, but it may produce microscopically visible alteration and its application in the narrow vertical bone defect is limited [10]. Mechanical debridement instruments made from plastic and other non-metals have been applied to avoid damaging titanium surfaces during instrumentation. However, these non-metallic instruments are ineffective for removing bacterial plaque and calcium depositions [11]. Removal of the adhered bacteria and their byproducts, such as LPS, on the dental implants has proven problematic because of the screw-shaped design and surface microstructure of implants [12]. The initial bacterial adhesion resides in the areas of high surface free energy and inside the pits and grooves of the roughened surfaces [13], which in turn accumulate more plaque. Moreover, the efficacy of debridement

* Corresponding author at: Institute of Oral Science, Chung Shan Medical University, Taichung City, 402, Taiwan.
** Corresponding author at: School of Dentistry, Chung Shan Medical University, Taichung City, 402, Taiwan.
E-mail addresses: sjding@csmu.edu.tw (S.-J. Ding), fw3256@gmail.com (C.-C. Chen).

https://doi.org/10.1016/j.pdpdt.2018.11.008
Received 25 August 2018; Received in revised form 3 November 2018; Accepted 9 November 2018
Available online 13 November 2018
1572-1000/

has varied in different clinical cases [14]. In addition, the etiopathogenesis of peri-implantitis is not well delineated [15]. Thus, the most effective treatment for peri-implantitis has not been conclusively established.

In an attempt to reduce the prevalence rate, antibiotic therapy is often recommended for patients receiving periodontitis and peri-implantitis treatment procedures. The use of systemic antibiotics as an adjunct in the treatment of periodontal disease is essential, but overuse of antibiotics has been a major culprit in the production of drug-resistant organisms. The increasing bacterial resistance to antibiotics adds to the demand for more specific methods for bacterial eradication like laser therapy [16]. Bacterial elimination using laser has been investigated previously and is considered an alternative therapeutic modality in periodontal therapy [10,17]. However, PDT may overcome the drawbacks of using high power laser, such as tissue damage, bone and pulpal lesions. The non-invasive aPDT to control biofilm formation/growth has attracted much interest [5,6,9]. The aPDT method applies the local delivery of visible light to living tissue, especially for irradiation of infected tissues previously exposed to a photosensitizer. The aPDT has emerged as an attractive alternative in the treatment of peri-implantitis to reduce bacteria and LPS adherent to titanium implant surface without causing damage of surface microstructure [18]. A series of studies have addressed that it is possible to kill bacteria with a light source from a low power laser after the microorganisms have been sensitized with a low concentration of photosensitizers, such as methylene blue (MB) [18–20] or toluidine blue O (TBO) [16]. Abduljabbar suggested that the mechanical debridement with adjunct aPDT was more effective in the treatment of peri-implant diseases compared with the mechanical debridement alone [21].

The most important component in aPDT process is photosensitizer. Methylene blue (MB) as a photosensitizer has been widely used for aPDT. Its concentration and pH are important factors for practical bactericidal applications. MB may induce either the formation of radical (type I) or singlet oxygen (type II) species, which the yield of singlet oxygen ($^1O_2$) depends on the pH of the medium [20]. In addition, MB-sensitized photolysis rates are higher at basic pH than acidic pH [22]. Thus, the solution pH used in the aPDT would be an evinced parameter for treatment of peri-implantitis on the dental implant. A search of the literature shows a paucity of articles addressing the effects of MB concentration, pH value of MB, and irradiation time on the eliminating efficacy of the infected titanium implants. It is worthy to verify the synergetic effect of the three factors during the aPDT process. In particular, systematic studies to explore aPDT in acid or alkaline environments on peri-implantitis therapy are still rare. Concerning the implant systems, SLA has always been used for the surface treatment of the commercially available titanium dental implants to increase the osseointegration [14,23] because the SLA-pretreated implants could possess a significantly high surface micro-roughness. However, the complex topography of the surface makes the peri-implantitis difficult to completely therapy. For this reason, in this work the SLA-pretreated Ti alloy was used as a substrate to investigate the antimicrobial efficacy of MB-mediated PDT. It is hypothesized that the appropriate MB concentration at optimal solution pH under a feasible irradiation time was effective at eradicating bacteria adhered on SLA-pretreated implant surfaces in vitro. Gram-negative (*P. gingivalis* and *A. actinomycetemcomitans*) and Gram-positive (*S. mutans*) bacteria were selected for investigating bacteria resistance to photoinactivation. Accordingly, a systematic analysis for the effect of MB concentration (50, 100, and 200 μg/mL) and pH (4, 7, and 10) for 30 and 60 s of irradiation time on the antimicrobial efficacy against three bacterial species was performed. The variations in the pH of the MB solution were examined after aPDT. More importantly, LPS levels remaining on the SLA-pretreated Ti surfaces were also evaluated because the biofilms inactivated/killed by aPDT could remain on the implant surface, which would facilitate subsequent microbial adhesion.

2. Material and methods

2.1. Preparation of titanium alloy

Commercially available 3 mm-thick Ti-6Al-4 V alloys (ASTM F136-84; Titanium Industries, Parsippany, NJ, USA) of 10 × 10 mm^2 were selected as the substrate materials. A total of 1655 Ti alloy plates were wet-ground with a 1200-grit SiC abrasive paper (3 M Wetordry TriMite 734, St. Paul, MN), followed by sandblasting with Al_2O_3 particles with 100 μm (Korox, Bego, Bremen, Germany) for 10 s. The air-pressure was 3.5 bar using a Taicrown P-002B machine (Taichung, Taiwan) and the distance between the orifice and the metal surface was approximately 10 mm. After that, the plates were followed by acid etching in HCl/H_2SO_4/H_2O (1:1:100) at 100 °C for 30 min to obtain SLA surface [10]. The SLA discs were then ultrasonically cleaned in acetone and ethanol for 20 min at each step, rinsed in deionized water, and then dried in an oven at 60 °C.

2.2. Bacterial adhesion

Gram-negative bacteria (*Porphyromonas gingivalis* (*P. gingivalis*, A7436) and *Aggregatibacter actinomycetemcomitans* (*A. actinomycetemcomitans*, IDH 781)) and Gram-positive bacteria (*Streptococcus mutans* (*S. mutans*, ATCC 700610) were used. Ti alloy specimens were placed in 24-well culture plates and 1 mL of bacteria was seeded on the specimens at a density of 2 × 10^6 colony-forming unit (CFU)/mL in Wilkins-Chalgren Anaerobe broth (Oxoid, Hampshire, UK) at 37 °C under anaerobic conditions for 24 h. The contaminated specimens were washed two times with phosphate buffer solution (PBS) for following photodynamic treatment.

2.3. Preparation of methylene blue

Methylene blue ($C_{16}H_{18}ClN_3S$; Riedel-deHaen Co, Buffalo, NY, USA) was used without further purification. The three concentrations of 50 (156 μM), 100 (312 μM), and 200 μg/mL (625 μM) MB solutions in phosphate buffer solution (PBS) were prepared. The pH of the MB solution was varied from 4 to 10 with a separation of 3 using drops of 1 N HCl or NaOH for prevention of large concentration changes when needed to achieve the desired pH [24]. The pH value of the MB solution was monitored with an IQ120 miniLab pH meter (San Diego, CA, USA).

2.4. Photodynamic treatment

After culture for 24 h on 24-well culture plates, the contaminated specimens were sprayed with 100 μL of MB for reaction of 1 min and then washed by PBS. After which, the specimens were irradiated with the diode laser (Aculas-HB, Konftec, New Taipei City, Taiwan) with maximum output 80 mW working at 660 nm for 30 and 60 s, corresponding to fluencies of 2.4 and 4.8 J/cm^2, respectively. The distance between the irradiated specimen and the laser tip with 1 cm diameter was 10 mm at an incidence angle of 90°.

2.5. Determination of pH value

To verify the variation in the pH of the MB solution, the pH was examined using an IQ120 miniLab pH meter following aPDT for 60 s after the contaminated specimens were sprayed with 100 μL of MB for reaction of 1 min. The solution pH on the uncontaminated SLA discs was also detected as a control after aPDT for 60 s. Five measurements were carried out for each group, and the results were expressed as the mean ± standard deviation.

2.6. Bacterial viability analysis

The decontamination effectiveness of aPDT on bacterial species was

determined using an alamarBlue (Invitrogen, Grand Island, NY, USA) assay that was used for real-time and repeated monitoring of bacterial viability. The number of viable bacteria can be estimated via redox reactions between the fluorometric/colorimetric growth indicator dye of AlamarBlue and metabolically active bacteria. The alamarBlue method is found to be much less labor intensive, which represents a higher throughput alternative to the classic type of CFU assay [25,26]. After the end of the laser treatment, 600 μL of solution at a ratio of 1:10 of Alamar Blue to broth was added to 24-well culture plates, followed by being incubated at 37 °C for 20 min. Subsequently, 100 μL of the solution in each well was transferred to a new 96-well tissue culture plate. Plates were read in a Sunrise Microtiter reader (Tecan Austria Gesellschaft, Salzburg, Austria) at 570 nm with a reference wavelength of 600 nm. The bacteria cultured on the Ti alloy surfaces without MB was used a control. The aPDT efficacy at different MB concentrations, pH solution, and irradiation time was expressed as the reduction ratio normalized to that of the control by means of the absorbance change [27]. The absorbance value used in this study can be proportional to the number of viable bacteria present. The reduction ratio (%) was calculated as follows: (absorbance of alamarBlue obtained on the control-absorbance of alamarBlue obtained on aPDT-treated specimens)/absorbance of alamarBlue obtained on the control) × 100%. The data provided for each group were the mean of fifteen independent measurements.

2.7. Morphology observation

To observe surface morphology on the specimen surfaces before and after aPDT, three specimens per group were washed three times with PBS and fixed in 2% glutaraldehyde (Sigma, St. Louis, MO, USA). The specimens were then dehydrated using a graded ethanol series for 20 min at each concentration. The dried specimens were mounted on stubs, coated with gold layer, and viewed using scanning electron microscopy (SEM; JEOL JSM-7800 F, Tokyo, Japan).

2.8. LPS detection

After aPDT, the remaining LPS concentrations on the substrates were quantified using a ToxinSensor chromogenic Limulus Amebocyte Lysate endotoxin assay kit (GenScript, Piscataway, NJ, USA) according to the manufacturer's instructions. The Ti alloy substrate with and without bacterial adhesion was used a positive and negative control, respectively. Five replicates were carried out for each group, and the results in terms of absorbance at 545 nm are expressed as the mean ± standard deviation.

2.9. Statistical analysis

All the results were expressed as the mean ± standard derivation for the total number of replicate experiments indicated unless otherwise stated. A one-way analysis of variance (ANOVA) was used to evaluate significant differences between the means. Scheffe's multiple comparisons were used to determine the significance of the standard deviations between the sample measurements under different experimental conditions. The result was considered statistically significant when the p-value was less than 0.05.

3. Results

3.1. Bacterial adhesion

Fig. 1a shows that there is the presence of etching-induced round shaped grooves on the SLA surface. After seeding bacterial species for 24 h, it can be clearly seen that the bacteria uniformly adhered to the surfaces (Fig. 1b-d). *S. mutans* was a short rod appearance (Fig. 1b). Gram-negative bacteria *A. actinomycetemcomitans* was close to rod-shaped (Fig. 1c) and *P. gingivalis* also presented a short rod-shaped morphology (F. 1d). Intriguingly, *P. gingivalis* had a lower amount on the SLA surface compared to the other two species at the same culture conditions.

3.2. pH variation

The solution pH (H^+ ion) fluxes could be associated with efficacy of aPDT. Thus, the variations of pH values in the MB medium during the photosensitization process deserved evaluation to elucidate the concerns raised. Fig. 2 shows the pH variations after aPDT treatment for 60 s following the culture on the contaminated implants for 24 h and on the control with the uncontaminated specimens. No obvious changes in pH were detected for the pH 4 and 7 groups on the uncontaminated specimens, while the aPDT treatment could reduce alkaline pH 10 down to about pH 9. When the pH was examined on *S. mutans-contaminated* and *A. actinomycetemcomitans*-contaminated surfaces, it remarkably turned pH from 4 to about 5.3, independent of MB concentration. Concerning *P. gingivalis*-contaminated surfaces, the MB concentration caused the acidic pH to increase, indicating the range from pH 4.3 to 5.1. In contrast, the initial alkaline pH reached a lower value of about pH 8.5 after aPDT for 60 s of treatment on the three contaminated surfaces. Interestingly, the neutral pH value was not changed over aPDT, even if various MB concentrations were used.

3.3. Bacterial viability

Fig. 3 shows the changes in the reduction percentage of the three bacterial species before and after the use of aPDT for 30 (2.4 J/cm^2) and 60 sec (4.8 J/cm^2), in combination with different MB concentrations as a function of solution pH. In the case of lack of aPDT, it seems that the decontamination ability of both MB concentration and pH factors against the three species was bacteria-dependent, which indicated the reduction ratio of *A. actinomycetemcomitans* had a lower value than the other bacterial species (Fig. 3b). As expected, the decontamination efficacy increased significantly ($p < 0.05$) with increasing MB concentrations without aPDT. For example, the 200 μg/mL MB at pH 7 reduced appreciably about the number of 72% *S. mutans* whereas the 50 μg/mL MB at pH 7 eliminated 50% of the viable *S. mutans* (Fig. 3a). On the other hand, the reduction ratio of the bacterial species was affected to a small extent by pH 10, although the alkaline pH was in favor of eliminating *P. gingivalis* (Fig. 3c) compared to the other two bacterial species. Of note, the variations in solution pH did not give rise to the changes in the reduced number of *S. mutans*.

When MB-mediated aPDT was used, it showed significantly greater eradication efficacy with an increased time. The aPDT treatment could achieve up to 80% reduction of bacterial counts for all groups. Notably, the 60-sec irradiation time almost completely killed the three bacterial species, indicating no statistically significant difference ($p > 0.05$) in bacterial quantity among the concentration groups, except the pH 4 group against *S. mutans* (Fig. 3a). In contrast, bacteria were found on 30 s-treated groups that revealed no 100% reduction. It is no doubt that aPDT with higher MB concentration effectively killed the bacteria than obtained by using the lower concentration. On the basis of the results above, the following studies on the evaluation of remaining bacterial morphology observed by SEM and determined by residual LPS assay focused on the photosensitizer conditions of the 100 and 200 μg/mL MB at either pH 7 or 10.

3.4. Remaining bacterial morphology

To further clarify the effect of aPDT on the presence of bacteria on the contaminated surfaces, the remaining bacterial colonies on the Ti alloy surfaces was examined using SEM. The treatments effectively reduced the number of bacterial CFU, as shown in Figs. 3–5, when compared with the contaminated groups (Fig. 1). The results of SEM

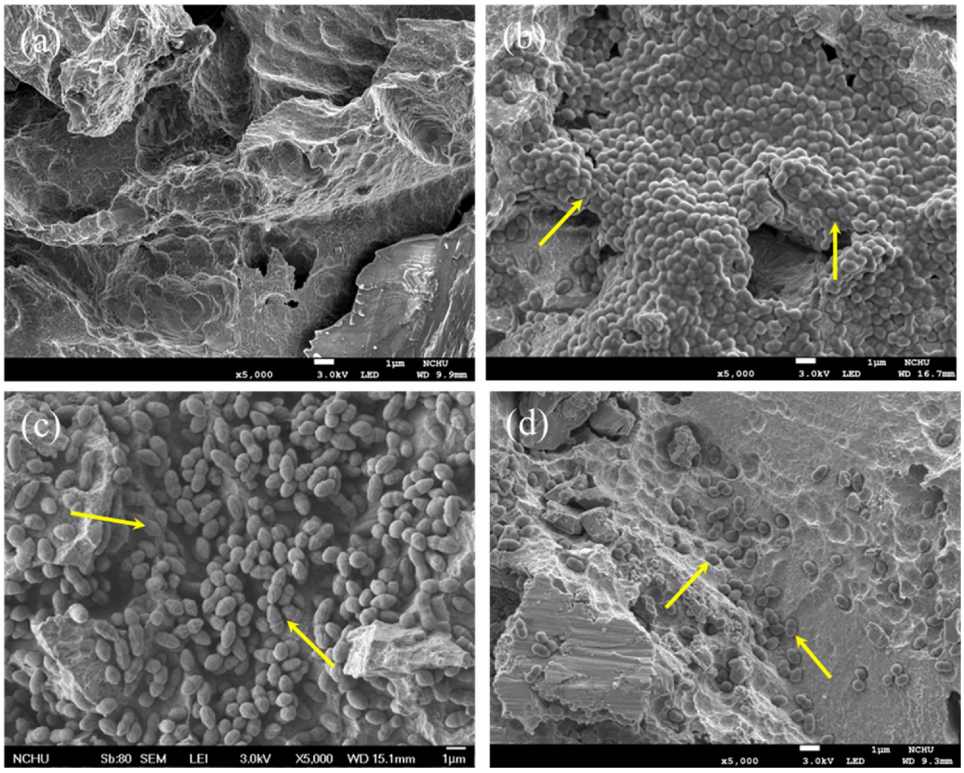

Fig. 1. Scanning electron micrographs of SLA-pretreated Ti alloy surfaces before (a) and after seeding with (b) *S. mutans*, (c) *A. actinomycetemcomitans*, and (d) *P. gingivalis* for 24 h. It can be clearly seen that the bacteria adhered to the surfaces. The arrows indicated the presence of bacteria.

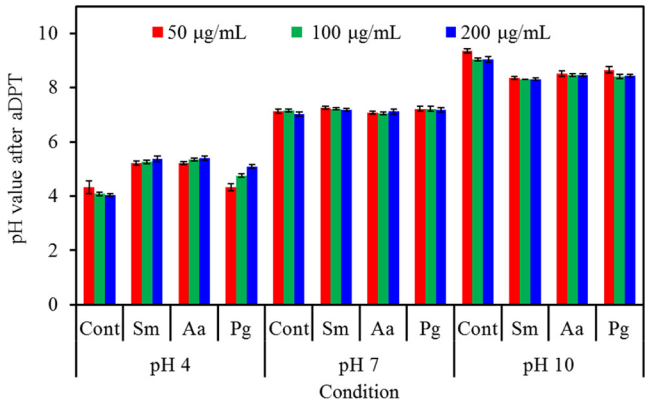

Fig. 2. Variations in the pH of different MB solutions during photosensitization process for 60 s when cultured with *S. mutans*, *A. actinomycetemcomitans*, and *P. gingivalis* under anaerobic conditions for 24 h. (Cont: the control without seeding bacteria; Sm: *S. mutans*; Aa: *A. actinomycetemcomitans*; Pg: *P. gingivalis*).

were in line with the results of the viability assay (Fig. 3). Concerning the bacterial species, in contrast to the findings in the *S. mutans*-contaminated (Fig. 4) and *A. actinomycetemcomitans*-contaminated (Fig. 5) surfaces, a complete removal of *P. gingivalis* adherent to the Ti surface was observed after PDT for 60 s (Fig. 6).

3.5. Residual LPS level

LPS is the major cell wall component of Gram-negative bacteria, such as *A. actinomycetemcomitans* and *P. gingivalis*. To investigate the removal of biofilms from the contaminated Ti alloy surfaces using aPDT, the amounts of residual LPS on the surfaces were examined. The negative control without bacteria culture indicated a relatively low LPS amount, while the positive control with contamination and PDT-free treatment presented a remarkably high LPS level, as shown in Fig. 7. Fig. 7a shows significant differences ($p < 0.05$) in residual LPS levels from *A. actinomycetemcomitans* when 100 μg/mL and 200 μg/mL MB were used. In addition, the alkaline pH solution resulted in a significantly lower ($p < 0.05$) residual LPS amount than those obtained from the corresponding groups at the neutral pH solution. Of note, the 60 s of irradiation time produced a significant increase ($p < 0.05$) in the removal of LPS from *A. actinomycetemcomitans* when compared with the 0 s and 30 s-treated groups. Residual LPS level on the *P. gingivalis*-contaminated surfaces revealed similar tendency with those on *A. actinomycetemcomitans*-contaminated surfaces before and after PDT (Fig. 7b). However, PDT with the 200 μg/mL MB had an appreciably low LPS level that was close to the negative control, which indicated the biofilm formed on the *P. gingivalis*-contaminated surfaces were almost completely eliminated, even if the neutral pH solution was used.

4. Discussion

There is an increasing demand to find efficient treatment modalities of peri-implantitis. Since aPDT plays an effective role in removal of contaminated Ti implants, some independent factors related to bactericidal effects of aPDT need to be demonstrated separately before the clinical applications. A variety of factors such as photosensitizer concentration, solution pH, irradiation time (light dose), laser type and bacterial species may dominate the bactericidal effect of aPDT [19,28–33]. The current study investigated the in vitro efficacy of MB-mediated aPDT with different MB concentrations and the pH of the solution against the reduction of viable bacteria and residue LPS adherent to SLA-pretreated titanium surface mimicking the bone-implant interface. Three different bacterial species were used to optimize the antimicrobial efficacy of aPDT parameters. Gram-negative *P. gingivalis* is associated with periodontitis and also implicated in peri-implantitis [2], whereas Gram-negative *A. actinomycetemcomitans* microaerophilic bacteria are one of the causative agents of periodontal disease [24]. *S. mutans* is an important bacterial stain in the initiation of dental caries

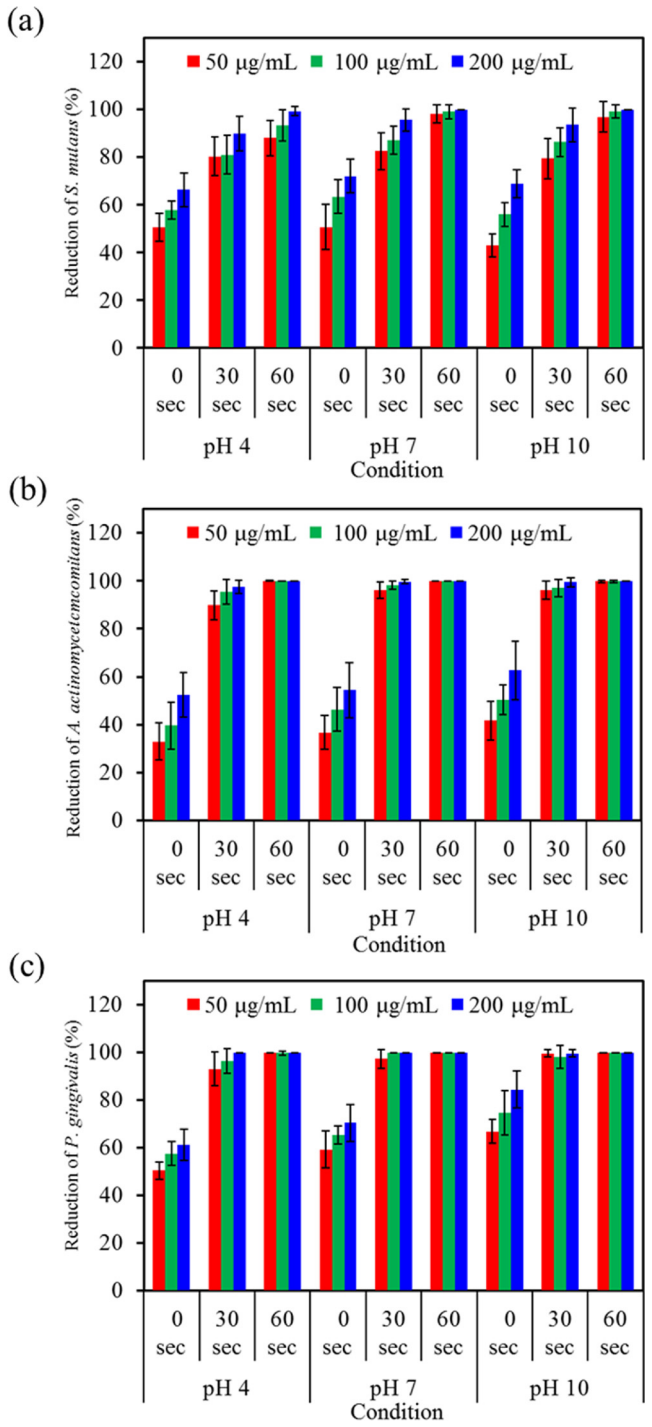

Fig. 3. The changes in the antimicrobial effectiveness of different concentrations of MB solutions differing by pH (4, 7, and 10) as a function of irradiation time against the reduction of (a) *S. mutans*, (b) *A. actinomycetemcomitans*, and (c) *P. gingivalis*.

[34].

A critical pathogenic event in the process of biofilm formation is bacterial adhesion on the implant surface [35]. It is worthy to observe the morphology and distribution of bacterial species adhered on the SLA implant surfaces after the culture for 24 h. In this study, the exposure of Ti surface to the bacterial suspension allowed the bacterial colonization that covered on the implant surface as proved by SEM images, viability assay, and LPS level. Different bacterial species displayed different amounts of CFU on the Ti surfaces. An alamarBlue assay was used to examine bacterial viability on the contaminated surfaces before and after aPDT at different experimental conditions. The results indicated that the greater MB concentration, the higher reductions of viable bacteria were found, consistent with the previous study [36]. MB alone attested concentration-dependent bactericidal activity against clinically relevant microorganisms at the pH value ranging from 4 to 10, which was due to possessing a broad spectrum of antibacterial activity [37,38]. Cationic photosensitizer MB can target bacterial membranes of both Gram-positive and Gram-negative bacteria and interact with anionic regions from bacterial cell walls [39]. MB could result in either strand breaks in the nucleic acid or cell envelope photodamage of Gram-negative bacteria [40]. It is reasonable to speculate that the bactericidal effects of MB could be different in bacterial species.

To assure to effectively eliminate the adhered bacteria, MB-mediated aPDT was suggested to use, instead of the MB alone. Indeed, the reduction ratios of the three viable bacteria were obviously higher in the MB-mediated aPDT groups compared to the MB alone. The use of 200 μg/mL MB-aPDT showed stronger inhibitory effects than the lower MB concentrations, consistent with the previous study [6]. In a study by Kashef et al. [29], aPDT mediated with 200 μg/mL MB against multidrug resistant *E. coli* showed the killing efficacy of 99.90%. On the other hand, fluence (light lose) is an important light parameter to affect the photosensitization efficacy. The increased light dose could increase the photocytotoxicity of MB [34]. Prates et al. [30] found that the fluence of 9 J/cm^2 resulted in 99.7% killing *A. actinomycetemcomitans* suspension, which was significant higher than 97.2% killing efficacy at a fluence of 5.4 J/cm^2. When the infected implants were irradiated for longer time such as 60 s, fewer CFU adhered on surfaces, presenting the exposure time-dependent (or light lose-dependence) efficacy of MB-based aPDT. Lima Leal et al. [32] reported total bacterial killing of *S. mutans* using a light emitting diode for the irradiation time of 2 min.

The bone lesion environment may have varying pH from a neutral pH of 7.4 to an acidic pH as low as 5.0 during clinical practice because of bacterial-induced local metabolic acidosis or tissue inflammation [27]. When treating infected area with pH lower than neutral pH, the pH of photosensitizer solution should be considered, as suggested by Baptista's group [20], since the pH of the solution may certainly influence the efficiency of type I and type II photosensitization mechanisms. By contrast, basic pH levels can inhibit most microorganisms, including resistant bacteria [3]. On that count, the varying pH in the MB solution during aPDT process might be a promising way for bacteria inactivation. It is thus indispensable to verify the effect of the solution pH on the elimination efficacy of PDT on the infected Ti implants. In the current study, it seems that the pH would affect the antimicrobial efficacy, which was dependent on the bacterial species. The higher pH value, the greater the eradication against *P. gingivalis* was revealed from the results of bacterial viability and residual LPS amount. Contrary to the finding, Gram-positive *S. mutans* can tolerate a larger variation of the pH environments compared to the other two species. *S. mutans* is a typical acido-genic and acid-tolerant oral bacterium involved in the processes of caries development, which forms a biofilm to promote bacterial adherence to the tooth surface [34]. Marsh et al. [41] reported that *S. mutans* could up-regulate a number of specific proteins and functions after exposure to sub-lethal pH values, which may enhance survival under acidic conditions such as those encountered in caries lesions. Nevertheless, a more effective killing effect could be achieved when using photosensitizer in an elevated concentration at a higher pH environment. Chen et al. [24] found that the rate of Gram-positive and Gram-negative bacteria inactivation by MB at pH 9 was 3–25 times higher than the rate at pH 5. They also demonstrated that the quantum yield of $^1O_2$ generated by MB was much higher in basic than in acidic pH MB photosensitizer. In fact, solution pH may affect the type of photosensitization mechanism, which at pH 5 the protonation of MB led mostly to $^3MBH^{2+}$ and at pH 9 a dominant $^3MB^+$ state was formed [20,24].

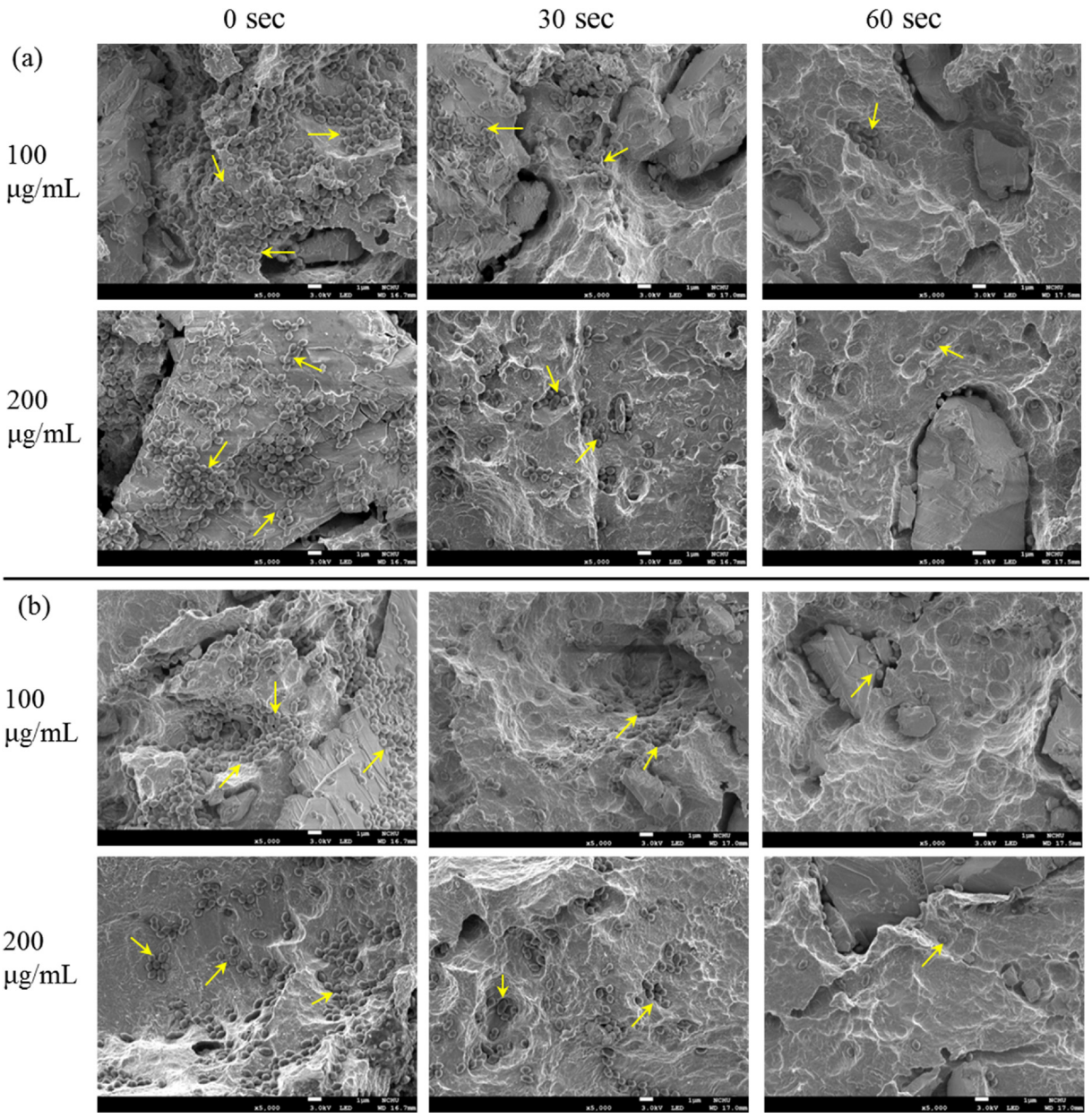

Fig. 4. Scanning electron micrographs of *S. mutans* on the infected surfaces after irradiation with 100 and 200 μg/mL MB at (a) pH 7 and (b) pH 10 for 0, 30, and 60 s. The arrows indicated *S. mutants*.

Given that the extracellular pH likely modulated aPDT to support bactericidal efficacy, it is important to quantify the pH variation when subjected to aPDT in the absence of bacteria. The current results indicated that both the acidic and neural pH values were almost maintained when it was limited to bacteria free experiments. Though not fully understood, it is interesting to note that MB can be deprotonated when the pH was elevated from 7 to 10 [24]. MB is normally present as a cation under physiological conditions, because of the presence of dimethylamino groups [33], which might result in the decreased pH. Nevertheless, their mechanisms still remained to be explored.

In a bacterial environment the variations in pH were also found during aPDT process, which depended on the initially environmental pH. In this study, the neutral pH was maintained after aPDT as found in the chemostat culture, while in the other the pH was allowed to change by bacterial metabolism. A remarkable increase in pH at acidic solution after aPDT on contaminated specimens for 60 s was detected, while the alkaline pH reduced. In other words, the solution pH revealed a trend toward the neutral pH after MB-mediated aPDT. One possibility is that this trend in the varying pH value, caused when aPDT treatment in the acidic or alkaline MB solution, would be pH homeostasis mechanism. Bacterial strains are capable of adapting to sub-lethal pH environments [42]. For example, the internal pH of *Escherichia coli* is maintained at 7.4–7.8 in media at pH 5.0–9.0 [43]. When the external pH exceeds 7.6, the pH homeostasis mechanism is inverted, i.e., the internal pH of the cell becomes more acidic than its environs. The maintenance of internal pH of microorganisms is important to the stability of macromolecules, which decarboxylases and deaminases play major roles in modulating cell response to pH changes [44,45]. Degradative decarboxylases neutralize the acidic external environment, whereas deaminases acidify the external environment by producing weak acids. This homeostasis leads to a drift of external pH toward neutrality [46].

Solution pH prompts an appreciable influence in formation of reactive oxygen species (ROS), such as $^1O_2$, superoxide anions, hydrogen peroxide and hydroxyl radicals [24]. PDT involves the interaction of a photosensitizer with light of an appropriate wavelength that, in the presence of molecular oxygen, generates toxic ROS, which are highly

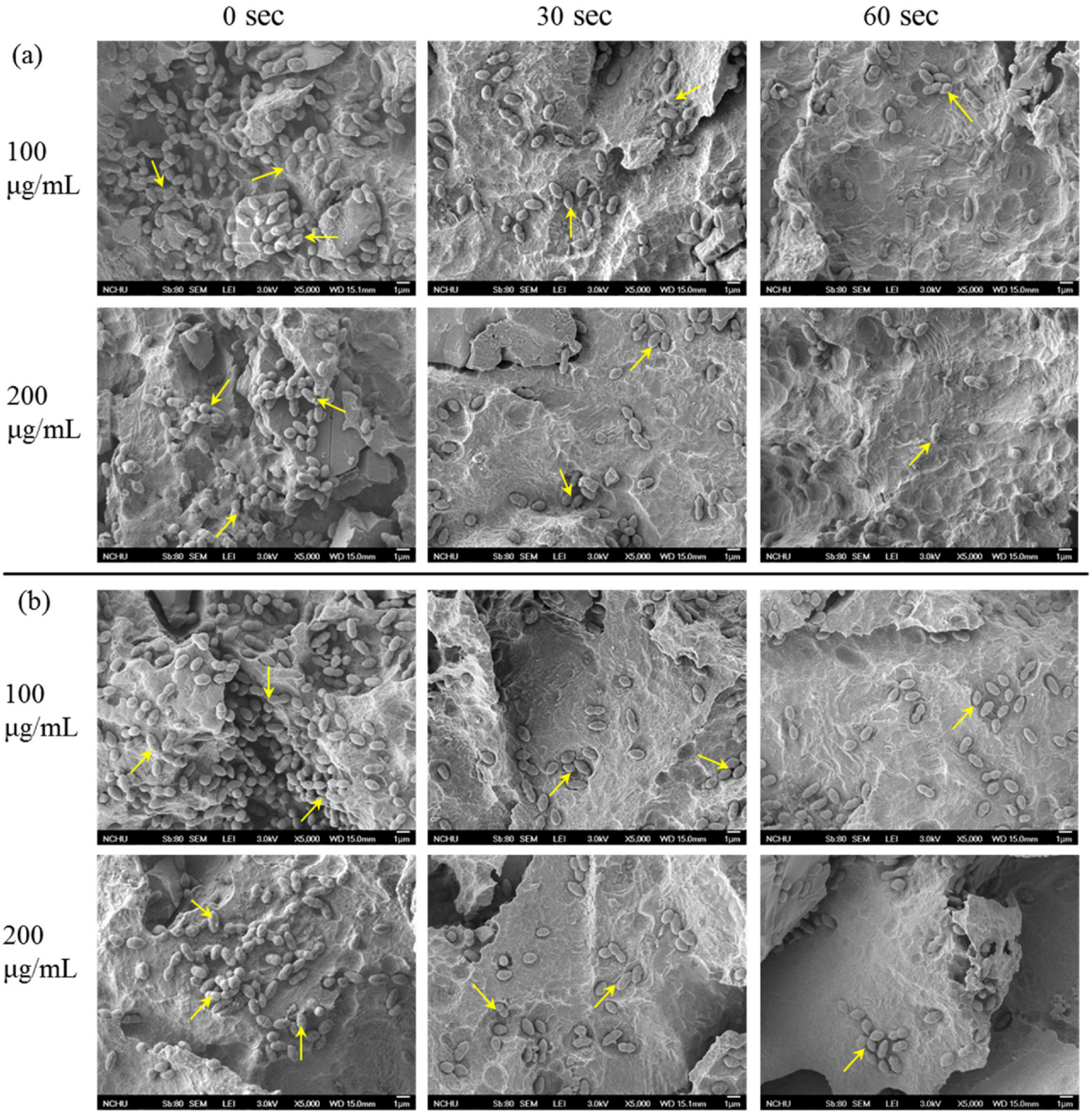

Fig. 5. Scanning electron micrographs of *A. actinomycetemcomitans* on the infected surfaces after irradiation with 100 and 200 μg/mL MB at (a) pH 7 and (b) pH 10 for 0, 30, and 60 s. The arrows indicated *actinomycetemcomitans*.

reactive and oxidize cellular substrates resulting in cell death by the induction of apoptosis or necrosis [47,48]. Although the solubility of molecular oxygen does not change with the pH [24], but the efficiency of $^1O_2$ is related to the pH of the medium. Bonneau et al. [49] reported that the production of $^1O_2$ was approximately five times more efficient in basic than in acidic medium, when MB was used in aerated solutions. The efficiency of a photosensitizer in generating ROS depended on the its intrinsic characteristics in aqueous solution [20,50]. According to the literature [51,52], rapid changes in extracellular pH are likely to modulate the activity of a number of physiologically important processes such as ROS production and permeability transition. It is pointed out that lack of protons in mitochondrial matrix favors ROS generation, whereas acidification of matrix strongly inhibits this process [51]. One possible explanation for the present results was that the alkaline pH 10 generated higher ROS upon aPDT, while at acidic pH 4 an insufficient amount was available to induce the observed photocytotoxic effect.

Although both viability assay and SEM observation consistently indicated the superior decontamination efficacy of aPDT on the Ti alloy surfaces, more detailed investigations such as LPS assay are crucial for understanding the roles of MB concentration and pH, and irradiation time. The biofilm-forming bacterial colonization on SLA-pretreated implants can never be completely avoided [53]. As expected, there was a relatively high LPS amount on the infected Ti alloy surface without any treatment, whereas the absorbance on the disinfected Ti surface displayed a detection limit of the endotoxin assay kit. The photosensitizer MB alone did reduce the residue LPS, consistent with the results of bacterial viability and SEM morphology. Alkaline pH solution also remarkably decreased the expression of the LPS compared to the neutral pH solution. After aPDT, the greater eradication efficacy was associated with elevated BM concentration at higher pH value and longer irradiation time. In the case of *A. actinomycetemcomitans*, the 200 μg/mL at pH 10 resulted in the significant decrease in the levels of residual LPS on the Ti surface among all groups. Interestingly, a greater reduction of LPS from *P. gingivalis*-contaminated titanium alloy surfaces was found than those from *A. actinomycetemcomitans*.

The current results of residual LPS level elucidated that *A.*

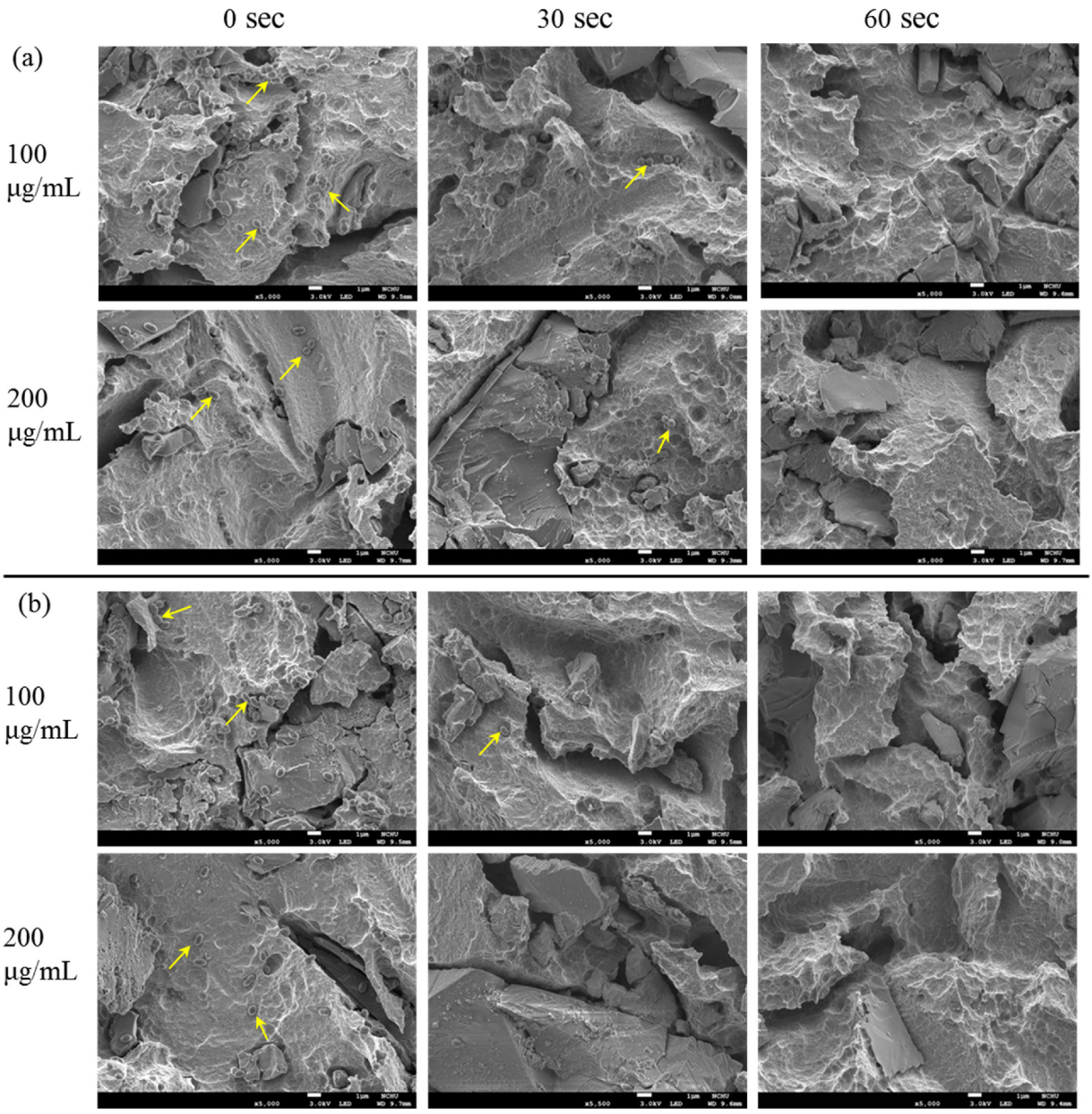

Fig. 6. Scanning electron micrographs of *P. gingivalis* on the infected surfaces after irradiation with 100 and 200 μg/mL MB at (a) pH 7 and (b) pH 10 for 0, 30, and 60 s. The arrows indicated *P. gingivalis*.

actinomycetemcomitans and *P. gingivalis* presented different susceptibilities towards aPDT, comparable to the previous studies [19,38,54]. Chan and Lai [19] found that *A. actinomycetemcomitans* was less sensitivity to PDT than *P. gingivalis* in the presence of MB. Similarly, Pfitzner et al. [54] reported that *P. gingivalis* was completely inactivated by PDT with photosensitizers including chlorin e6, BLC 1010, and BLC 1014, while low eradication effect was found for *A. actinomycetemcomitans* at the same applied energy density. The significant variations in removal of LPS between *A. actinomycetemcomitans* and *P. gingivalis* could be partly due to different structure of the bacteria [55]. This is due to the fact that the key feature of biofilms is the presence of an extracellular matrix, which contains a mixture of polymeric substances, including nucleic acids, proteins, and polysaccharides. Different bacterial species can produce different polymers and a single bacterial species has the capacity to produce several different exopolysaccharides [56], which may result in the different susceptibility to the antimicrobial therapy. In short, the results of the in vitro study revealed that it is possible to remarkably eliminate biofilm-associated bacterial populations using PDT with the 200 μg/mL MB at pH 10 for 60 s of irradiation time.

5. Conclusion

The focus of this study was to analyze the antimicrobial effect of PDT against Gram-positive and Gram-negative bacteria embarking on the optimization of treatment factors. Within the limitations of the in vitro study, MB-mediated PDT displayed the concentration-dependent, pH-dependent, and time-dependent efficacy of eradication therapy on biofilm-contaminated implant surfaces. The most effective killing occurred with exposure to laser light in combination with the 200 μg/mL MB photosensitizer at pH 10 for 60 s of irradiation time. However, further investigations, including the use of the multispecies biofilm model and the evaluation of in vitro osteogenesis, are required prior to the clinical application.

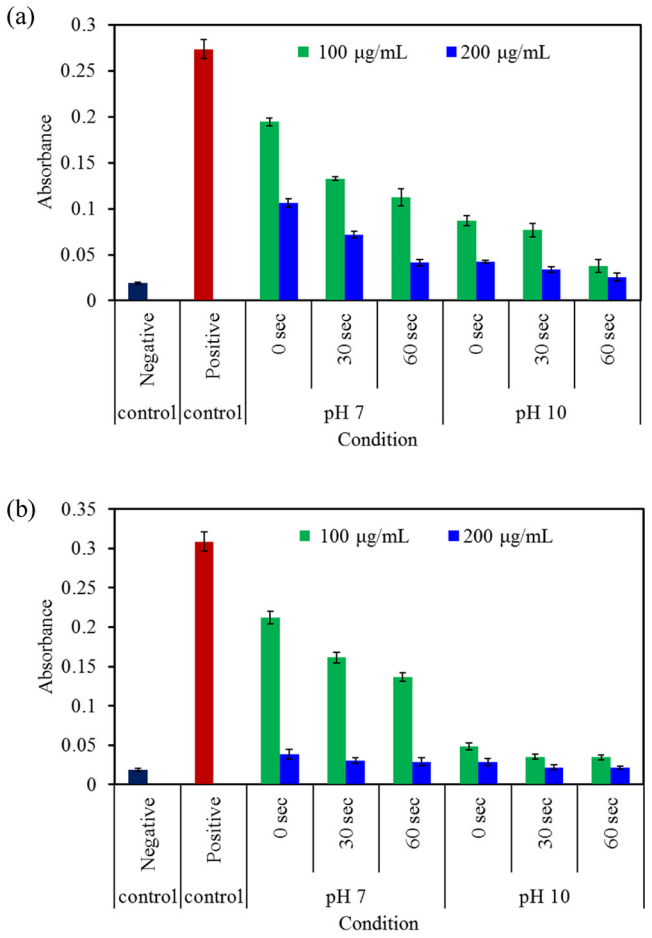

Fig. 7. Residual LPS levels from (a) *A. actinomycetemcomitans* and (b) *P. gingivalis* on infected surfaces subjected to various treatments. The Ti alloy substrate with and without bacterial adhesion was used a positive and negative control, respectively.

References

[1] A. Mombelli, N.P. Lang, The diagnosis and treatment of peri-implantitis, Periodontol. 2000 17 (1998) 63–76.

[2] A. Pier-Francesco, R.J. Adams, M.G.J. Waters, D.W. Williams, Titanium surface modification and its effect on the adherence of Porphyromonas gingivalis: an in vitro study, Clin. Oral Impl. Res. 17 (2006) 633–637.

[3] B.C. Wu, C.K. Wei, N.S. Hsueh, S.J. Ding, Comparative cell attachment, cytotoxicity and antibacterial activity of radiopaque dicalcium silicate cement and white-coloured mineral trioxide aggregate, Int. Endod. J. 48 (2015) 268–276.

[4] R.M. Donlan, J.W. Costerton, Biofilms: survival mechanisms of clinicallyrelevant microorganisms, Clin. Microbiol. Rev. 15 (2002) 167–193.

[5] L.J. Tavares, A.C. Pavarina, C.E. Vergani, E.D. de Avila, The impact of antimicrobial photodynamic therapy on peri-implant disease: what mechanisms are involved in this novel treatment? Photodiagn. Photodyn. Ther. 17 (2017) 236–244.

[6] M.A. Nemezio, S.S. de Souza Farias, M.C. Borsatto, C.P. Aires, S.A. Milori Coronac, Effect of methylene blue-induced photodynamic therapy on a *Streptococcus mutans* biofilm model, Photodiagn. Photodyn. Ther. 20 (2017) 234–237.

[7] N.U. Zitzmann, T. Berglundh, Definition and prevalence of peri-implant diseases, J. Clin. Periodontol. 35 (2008) 286–291.

[8] Y.C. de Waal, A.J. van Winkelhoff, H.J. Meijer, G.M. Raghoebar, E.G. Winkel, Differences in peri-implant conditions between fully and partially edentulous subjects: a systematic review, J. Clin. Periodontol. 40 (2013) 266–286.

[9] J. Marotti, P. Tortamano, S. Cai, M.S. Ribeiro, J.E.M. Franco, T.T. de Campos, Decontamination of dental implant surfaces by means of photodynamic therapy, Lasers Med, Sci. 28 (2013) 303–309.

[10] C.J. Chen, S.J. Ding, C.C. Chen, Effects of surface conditions of titanium dental implants on bacterial adhesion, Photomed. Laser Surg. 34 (2016) 379–388.

[11] S. Renvert, I. Polyzois, R. Maguire, Re-osseointegration on previously contaminated surfaces: a systematic review, Clin. Oral Impl. Res. 20 (2009) 216–227.

[12] M.H. Zablotsky, D.L. Diedrich, R.M. Meffert, Detoxification of endotoxin-contaminated titanium and hydroxyapatite-coated surfaces utilizing various chemotherapeutic and mechanical modalities, Implant Dent. 1 (1992) 154–158.

[13] W. Teughels, N. Van Assche, I. Sliepen, M. Quirynen, Effect of material characteristics and or surface topography on biofilm development, Clin. Oral Impl. Res. 17 (2006) 68–81.

[14] A. Louropoulou, D.E. Slot, F.A. van der Weijden, Titanium surface alterations following the use of different mechanical instruments: a systematic review, Clin. Oral Impl. Res. 23 (2012) 643–658.

[15] S. Jankovic, Z. Aleksic, B. Dimitrijevic, V. Lekovic, P. Camargo, B. Kenney, Prevalence of human cytomegalovirus and Epstein-Barr virus in subgingival plaque at peri-implantitis, mucositis and healthy sites. A pilot study, Int. J. Oral Maxillofac. Surg. 40 (2011) 271–276.

[16] M.N. Usacheva, M.C. Teichert, M.A. Bie, Comparison of the methylene blue and toluidine blue photobactericidal efficacy against Gram-positive and Gram-negative microorganisms, Lasers Surg. Med. 29 (2001) 165–173.

[17] M. Kreisler, W. Kohnen, A.B. Christoffers, H. Götz, B. Jansen, H. Duschner, B. d'Hoedt, In vitro evaluation of the biocompatibility of contaminated implant surfaces treated with an Er:YAG laser and an air powder system, Clin. Oral Impl. Res. 16 (2005) 36–43.

[18] M. Giannelli, G. Landini, F. Materassi, F. Chellini, A. Antonelli, A. Tani, D. Nosi, S. Zecchi-Orlandini, G.M. Rossolini, D. Bani, Effects of photodynamic laser and violet-blue led irradiation on *Staphylococcus aureus* biofilm and *Escherichia coli* lipopolysaccharide attached to moderately rough titanium surface: in vitro study, Lasers Med. Sci. 32 (2017) 857–864.

[19] Y. Chan, C.H. Lai, Bactericidal effects of different laser wavelengths on periodontopathic germs in photodynamic therapy, Lasers Med. Sci. 18 (2003) 51–55.

[20] J.P. Tardivo, A.D. Giglio, C.S. de Oliveira, D.S. Gabrielli, H.C. Junqueira, D.B. Tada, D. Severino, R.F. Turchiello, M.S. Baptista, Methylene blue in photodynamic therapy: from basic mechanisms to clinical applications, Photodiagn. Photodyn. Ther. 2 (2005) 175–191.

[21] T. Abduljabbar, Effect of mechanical debridement with and without adjunctantimicrobial photodynamic therapy in the treatment of peri-implantdiseases in prediabetic patients, Photodiagn. Photodyn. Ther. 17 (2017) 9–12.

[22] R.J. Watts, V.D. Adams, E. Middlebrooks, Effect of pH on the indirect photolysis treatment of three refractory herbicides, J. Chemosphere 17 (1988) 2083–2091.

[23] I. Abrahamsson, T. Berglundh, E. Linder, N.P. Lang, J. Lindhe, Early bone formation adjacent to rough and turned endosseous implant surfaces. An experimental study in the dog, Clin. Oral Impl. Res. 15 (2004) 381–392.

[24] J. Chen, T.C. Cesario, P.M. Rentzepis, Effect of pH on methylene blue transient states and kinetics and bacteria photoinactivation, J. Phys. Chem. A 115 (2011) 2702–2707.

[25] L.E. DeForge, K.L. Billeci, S.M. Kramer, Effect of IFN-γ on the killing of S. aureus in human whole blood: Assessment of bacterial viability by CFU determination and by a new method using alamarBlue, J. Immunol. Methods 245 (2000) 79–89.

[26] T. Kuda, T. Yano, Colorimetric alamarBlue assay as a bacterial concentration and spoilage index of marine foods, Food Control 14 (2003) 455–461.

[27] C.K. Wei, S.J. Ding, Dual-functional bone implants with antibacterial ability and osteogenic activity, J. Mater. Chem. B 5 (2017) 1943–1953.

[28] L.H. Alvarenga, R.A. Prates, T.M. Yoshimura, I.T. Kato, L.C. Suzuki, M.S. Ribeiro, L.R. Ferreira, S.A. dos Santos Pereira, E.F. Martinez, E. Saba-Chujfi, *Aggregatibacter actinomycetemcomitans* biofilm can be inactivated by methylene blue-mediated photodynamic therapy, Photodiagn. Photodyn. Ther. 12 (2015) 131–135.

[29] N. Kashef, G. Ravaei Sharif Abadia, G.E. Djavid, Phototoxicity of phenothiazinium dyes against methicillin-resistant *Staphylococcus aureus* and multi-drug resistant *Escherichia coli*, Photodiagn. Photodyn. Ther. 9 (2012) 11–15.

[30] R.A. Prates, A.M. Yamada, L.C. Suzuki, M.C.E. Hashimoto, S. Cai, S. Gouw-Soares, L. Gomes, M.S. Ribeiro, Bactericidal effect of malachite green and red laser on Actinobacillus Actinomycetemcomitans, J. Photochem. Photobiol. B 86 (2007) 70–76.

[31] E. Buytaert, M. Dewaele, P. Agostinis, Molecular effectors of multiple cell death pathways initiated by photodynamic therapy, Biochim. Biophys. Acta 1776 (2007) 86–107.

[32] C.R. Lima Leal, L.H. Alvarenga, T. Oliveira-Silva, I.T. Kato, B. Godoy-Miranda, S.K. Bussadori, M.S. Ribeiro, R.A. Prates, Antimicrobial photodynamic therapy on Streptococcus mutans is altered by glucose in the presence of methylene blue and red LED, Photodiagn. Photodyn. Ther. 19 (2017) 1–4.

[33] Mark Wainwright, David A. Phoenix, Lesley Rice, Shuna M. Burrow, Jack Warin, Increased cytotoxicity and phototoxicity in the methylene blue series via chromophore methylation, J. Photochem. Photobiol. B 40 (1997) 233–239.

[34] S. Hamada, T. Koga, T. Ooshima, Virulence factors of Streptococcus mutans and dental caries prevention, J. Dent. Res. 63 (1984) 407–411.

[35] J. Gallo, M. Holinka, C.S. Moucha, Antibacterial surface treatment for orthopaedic implants, Int. J. Mol. Sci. 15 (2014) 13849–13880.

[36] T. Briggs, G. Blunn, S. Hislop, R. Ramalhete, C. Bagley, D. McKenna, M. Coathup, Antimicrobial photodynamic therapy—a promising treatment for prosthetic joint infections, Lasers Med, Sci. 33 (2018) 523–532.

[37] M. Wainwright, K.B. Crossley, Methylene blue: a therapeutic dye for all seasons? J. Chemother. 14 (2002) 431–443.

[38] M. Umeda, A. Tsuno, Y. Okagami, F. Tsuchiya, Y. Izumi, I. Ishikawa, Bactericidal effects of a high-power, red light-emitting diode on two periodontopathic bacteria in antimicrobial photodynamic therapy in vitro, J. Investig. Clin. Dent. 2 (2011) 268–274.

[39] T. Berglundh, L. Persson, B. Klinge, A systematic review of the incidence of biological and technical complications in implant dentistry reported in prospective longitudinal studies of at least 5 years, J. Clin. Periodontol. 29 (2002) 197–212.

[40] M. Wainwright, Photodynamic antimicrobial chemother-apy (PACT), J. Antimicrob. Chemother. 42 (1998) 13–28.

[41] P.D. Marsh, Dental plaque as a biofilm and a microbial community – implications for health and disease, BMC Oral Health 6 (2006) S14.

[42] M. Goodson, R.J. Rowbury, Habituation to normally lethal acidity by prior growth of Escherichia coli at a sub-lethal acid pH value, Lett. Appl. Microbiol. 8 (1989) 77–79.
[43] J.L. Slonczewski, J.W. Foster, pH regulated genes and survival at extreme pH, in: F.C. Neidhardt (Ed.), Escherichia coli and Salmonella: Cellular and Molecular Biology, 2nd, ASM Press, Washington, 1996, pp. 1539–1550.
[44] M. Sharma, P.J. Taormina, L.R. Beuchat, Habituation of foodborne pathogens exposed to extreme pH conditions: genetic basis and implications in foods and food processing environments, Food Sci. Technol. Res. 9 (2003) 115–127.
[45] E.F. Gale, H.M.R. Epps, The effect of the pH of the medium during growth on the enzymic activities of bacteria (*Escherichia coli* and *Micrococcus lysodeikticus*) and the biological significance of the changes produced, Biochem. J. 36 (1942) 600–618.
[46] I.R. Booth. Regulation of cytoplasmic pH in bacteria, Microbiol. Rev. 49 (1985) 359–378.
[47] M. Triesscheijn, P. Baas, J.H. Schellens, F.A. Stewart, Photodynamic therapy in oncology, Oncologist 9 (2006) 1034–1044.
[48] J. Imlay, S. Linn, DNA damage and oxygen radical toxicity, Science 240 (1988) 1302–1309.
[49] R. Bonneau, R. Pottier, O. Bagno, J. Joussot-Dubien, pH dependence of singlet oxygen production in aqueous solutions using thiazine dyes as photosensitizers, Photochem. Photobiol. 21 (1975) 159–163.
[50] E. Gross, B. Ehrenberg, F.M. Johnson, Singlet oxygen generation by porphyrins and the kinetics of 9,10-dimethylanthracene photosensitization in liposomes, Photochem. Photobiol. 57 (1993) 808–813.
[51] V.A. Selivanov, J.A. Zeak, J. Roca, M. Cascante, M. Trucco, T.V. Votyakova, The role of external and matrix ph in mitochondrial reactive oxygen species generation, J. Biol. Chem. 283 (2008) 29292–29300.
[52] P.I. Milner, R.J. Wilkins, J.S. Gibson, The role of mitochondrial reactive oxygen species in pH regulation in articular chondrocytes, Osteoarthr. Cartil. 15 (2007) 735–742.
[53] C.J. Chen, C.C. Chen, S.J. Ding, Effectiveness of hypochlorous acid to reduce the biofilms on titanium alloy surfaces in vitro, Int. J. Mol. Sci. 17 (2016) 1161, https://doi.org/10.3390/ijms17071161.
[54] A. Pfitzner, B.W. Sigusch, V. Albrecht, E. Glockmann, Killing of periodontopathogenic bacteria by photodynamic therapy, J. Periodontol. 75 (2004) 1343–1349.
[55] J. Fyrestam, N. Bjurshammar, E. Paulsson, N. Mansouri, A. Johannsen, C. Östman, Influence of culture conditions on porphyrin production inAggregatibacter actinomycetemcomitans and Porphyromonas gingivalis, Photodiagn. Photodyn. Ther. 17 (2017) 115–123.
[56] L. Friedman, R. Kolter, Two genetic loci produce distinct carbohydrate-rich structural components of the pseudomonas aeruginosa biofilm matrix, J. Bacteriol. 186 (2004) 4457–4465.